ACS Sustainable Chemistry & Engineering

Research Article

pubs.acs.org/journal/ascecg

RGO/ZnO Nanocomposite: An Efficient, Sustainable, Heterogeneous, Amphiphilic Catalyst for Synthesis of 3-Substituted Indoles in Water

U. Chinna Rajesh,[†] Jinfeng Wang,[‡] Stuart Prescott,[§] Takuya Tsuzuki,*[,∥] and Diwan S. Rawat*[,†]

[†]Department of Chemistry, University of Delhi, Delhi 110007, India

[‡]Institute for Frontier Materials, Deakin University, Geelong, Victoria 3217, Australia

[§]School of Chemical Engineering, UNSW Australia, Sydney, NSW 2052, Australia

[∥]Research School of Engineering, College of Engineering and Computer Science, Australian National University, Ian Ross Building 31, North Road, Canberra ACT-0200, Australia

Supporting Information

ABSTRACT: A nanocomposite consisting of reduced graphene oxide and zinc oxide nanoparticles (RGO/ZnO) with unique structural features was developed as an efficient, sustainable, amphiphilic, heterogeneous catalyst for the synthesis of various 3-substituted indoles in water. The catalyst was recycled six times without significant loss in catalytic activity. The higher environmental compatibility and sustainability factors such as smaller E-factor and higher atom economy make the present methodology a true green and sustainable process for the synthesis of various biologically important 3-substituted indoles.

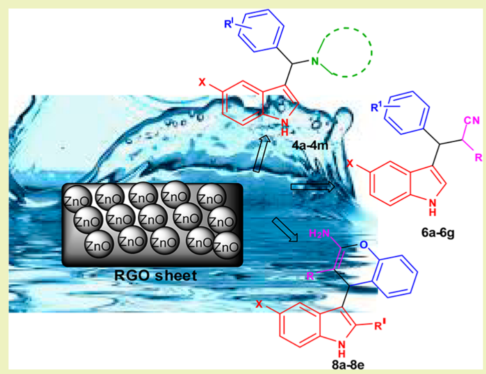

KEYWORDS: *RGO/ZnO nanocomposite, Amphiphilic catalyst, E-factor, Atom economy, Green, Sustainable, 3-Substituted indoles*

INTRODUCTION

Recently, research on graphene and other two-dimensional sp^2-hybridized carbon nanomaterials has attracted strong scientific and technological interest in the areas of physics, engineering, materials science, and modern chemistry.[1−3] In particular, graphene-based materials such as graphene oxide (GO) and reduced graphene oxide (RGO) have attracted significant attention because of their unique properties that are suitable for various applications including sensors,[4] supercapacitors,[5] pollutant adsorbents,[6] and catalysts.[7,8]

Catalysis with graphene-based materials in organic transformations is an important and relatively new research area with outstanding potential for industrial applications. However, very limited reports have been found on the applications of GO, RGO, or its composite materials as heterogeneous catalysts in organic conversions. Bielawski and co-workers demonstrated that the acidic nature of GO was responsible for oxidation and hydration reactions.[9] RGO and Au/graphene hydrogels were used as catalysts for the reduction of a variety of substituted nitrobenzenes to the corresponding anilines.[10,11] Scheuermann et al. impregnated GO/RGO with palladium nanoparticles and used them as catalysts in Suzuki−Miyaura coupling reactions.[12] RGO/ZnO nanocomposites have applications in diverse fields such as electrochemical capacitors,[13] adsorbents for pollutants and removal of RhB dye from water,[14] photocatalysts, and fabrication of organic photovoltaics.[15,16] Although ZnO nanoparticles (NPs) alone have been explored as heterogeneous catalysts for organic transformations,[17,18] RGO/ZnO nanocomposites have not been investigated in catalysis.

Heterogeneous catalysis in water as a solvent is considered a green and sustainable approach because water is the safest solvent and reduces the environmental factor (E-factor). Water is also known to enhance the rate and selectivity of organic reactions due to interactions like hydrogen bonding, hydrophobic effect, polarity, and trans-phase interactions.[19,20] Furthermore, the "Breslow effect" can increase the rate of organic reaction in water, wherein the hydrophobic aggregation of organic molecules decreases the area of the nonpolar surface and in turn reduces the activation energies.[21] Another approach to overcome the problem of low solubility of organic substrates in water is to use amphiphilic catalysts.[22] In this context, we presumed that RGO/ZnO composites can act as amphiphilic heterogeneous recyclable catalysts in water, as the RGO surface is hydrophobic and the surface polarity of ZnO NPs is hydrophilic in nature.[23,24] Thus, RGO/ZnO composites may overcome the mass transfer limitation in water by enlarging the accessibility of organic molecules near the RGO surface.

Indole frameworks have been found in various biologically active natural products, agrochemicals and pharmacological relevance molecules.[25,26] Among these, 3-substituted indoles

Received: May 10, 2014
Revised: November 18, 2014
Published: November 21, 2014

are of special interest as medicinally potent lead molecules and a key intermediate for the synthesis of various therapeutic agents.[27,28] 3-Substituted indoles can be synthesized from the reaction between benzaldehyde, secondary/primary amines, and indole via Mannich-type reactions.[29−31] 2-((*1H*-Indol-3-yl)(phenyl)methyl)malononitriles and 2-amino-4-(indol-3-yl)-*4H*-chromenes have been reported by the reaction of indole, active methylene compounds, and benzaldehyde/2-hydroxy benzaldehyde in the presence of a few homogeneous catalysts such as the copper(II) sulfonato salen complex, Zn(salphen) complex, N,N^{II}-dioxide Zn(II) complex, and TBAF.[32−35] However, these methods suffer from drawbacks such as the usage of organic solvents, complicate workup procedures, long reaction times, and expensive nonrecyclable catalysts, which has a high E-factor with low environmental compatibility. Therefore, the development of efficient heterogeneous catalytic systems for the environmentally benign synthesis of 3-substituted indole derivatives remains a challenging task. As a part of our continuing efforts on designing novel recyclable catalysts[36−39] for important organic transformations and synthesis of medicinally important molecules,[40−42] we report RGO/ZnO nanocomposites as novel and efficient recyclable heterogeneous amphiphilic catalysts for synthesis of various 3-substituted indoles in water.

■ RESULTS AND DISCUSSION

The RGO/ZnO composites were prepared using the method reported in our earlier study.[43] Figure 1 shows a typical transmission electron microscopy (TEM) image of the RGO/ZnO nanocomposites. It is evident that ZnO NPs were well dispersed on the surface of the RGO nanosheets.

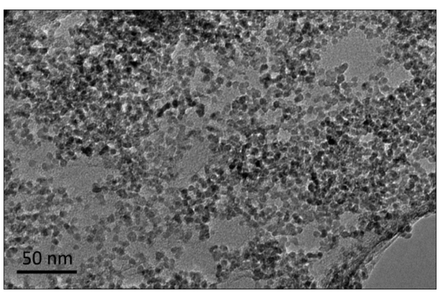

Figure 1. Transmission electron micrograph of RGO/ZnO nanocomposites.

The hydrophilicity of RGO/ZnO and GO/ZnO nanocomposites was examined by using water contact angle (CA) measurements as shown in Figure 2. The results revealed that RGO/ZnO showed a hydrophilic nature with a water static contact angle of 74° (Figure 2b). However, the hydrophilicity of the RGO/ZnO composite was comparatively less than the GO/ZnO composite, which showed a water static contact angle of 55° (Figure 2a).

The weight ratio of graphene oxide (GO) to ZnO was measured in our earlier study using thermogravimetric analysis (TGA) and was found to be 43.2 wt % (GO) and 52 wt % (ZnO), and the remaining 4.3 wt % was from poly(vinylpyrrolidone) (PVP).[43] The concentration of acidic sites of GO/ZnO was calculated using a titration method and was found to be 26 mmol/g.

The specific surface area of the GO/ZnO was measured by the NMR solvent relaxation method and was found to be 150 m^2/g. The results clearly showed that the solvent accessible surface area of the system is dominated by the ZnO component, and it can be concluded that to a reasonably approximation the total specific surface area of the GO/ZnO composite is the same as that of the ZnO NPs (Figure 3).

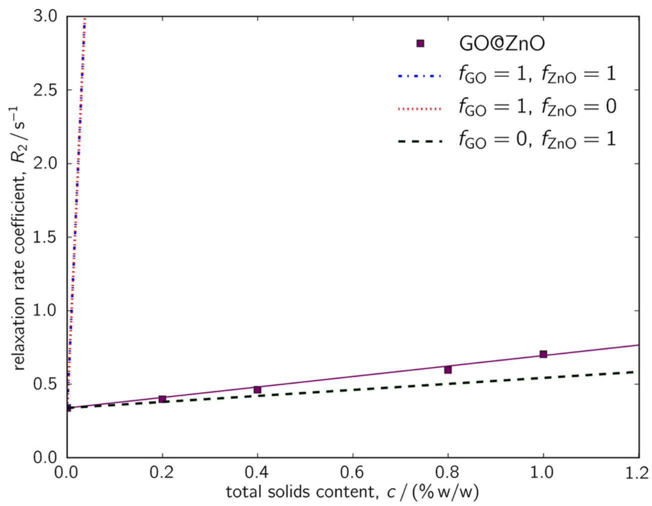

Figure 3. NMR solvent relaxation rates for the GO/ZnO composite.

As shown in Figure 3, the relaxation rate enhancement of ZnO is sufficiently weak so that the first two scenarios lie on top of each other. The comparison of the experimental data for dispersions of GO/ZnO with the predictions for the limiting scenarios indicates that while none of them exactly match the experiment there is very little GO surface that is solvent accessible in the time scales of the NMR experiment. Additional

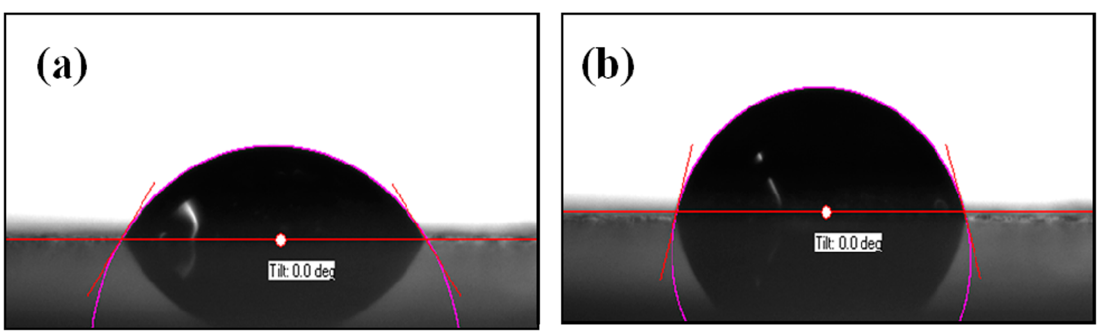

Figure 2. Water contact angle on surfaces of (a) GO/ZnO and (b) RGO/ZnO. Red line is the droplet baselines from which the contact angles were determined.

dx.doi.org/10.1021/sc500594w | ACS Sustainable Chem. Eng. 2015, 3, 9−18

Scheme 1. RGO/ZnO-Catalyzed Synthesis of 3-Amino Alkylated Indoles in Water

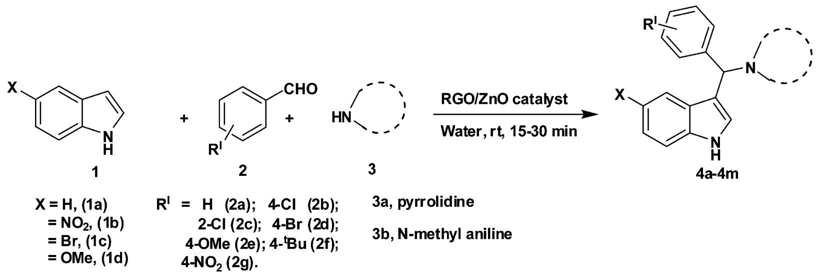

scenarios can be added to the analysis shown in Figure 3; however, gradients intermediate between that of the GO and ZnO samples do not have unique solutions.

On the basis of the above observation that the sensitivity of the GO is quite high (Figure S1, Supporting Information) compared to the sensitivity to ZnO (Figure S2, Supporting Information); any intermediate scenarios will show a very small value for f_{GO}, indicating that very little of the GO surface is solvent accessible. One such intermediate scenario is shown in Figure 3, in which $f_{ZnO} = 1$ and $f_{GO} = 2 \times 10^{-3}$.

Catalytic Applications of RGO/ZnO Composite. The catalytic activity of RGO/ZnO was investigated in the synthesis of various 3-substituted indoles. Initially, the catalytic potential of RGO/ZnO composites was examined in a model reaction of indole, benzaldehyde, and pyrrolidine to obtain 3-amino alkylated indole **4a** using 5 wt % of RGO/ZnO catalyst in various solvents at room temperature (Scheme 1).

As shown in Table 1, in the presence of organic solvents, the reaction proceeded slowly and resulted in the formation of product **4a** in poor yields (Table 1, entries 1−4). When water was used as a solvent, the product formation enhanced rapidly with 90% yield in a short reaction time of 20 min (Table 1, entry 5). We carried out the model reaction in the presence of GO as a catalyst under optimized conditions, and a trace amount of product was formed after prolonged reaction time (entry 6). In the presence of commercially available nanoZnO as a catalyst, product **4a** was obtained in 70% yield (Table 1, entry 7). The reaction did not proceed in the absence of the catalyst even after a prolonged reaction time of 240 min (Table 1, entry 9). This indicates that the RGO/ZnO catalyst plays a significant role in the synthesis of 3-amino alkylated indole **4a**.

Table 1. Optimization Study for RGO/ZnO Catalyzed One-Pot Mannich-Type Reactions[a]

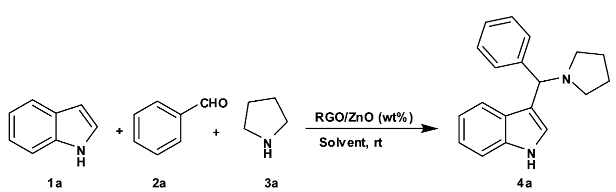

entry	solvent	catalyst (5 wt %)	time (min)	yield of **4a** (%)[c]
1	DMSO	RGO/ZnO	120	40
2	CH_3CN	RGO/ZnO	120	45
3	acetone	RGO/ZnO	120	30
4	THF	RGO/ZnO	120	40
5	**water**	**RGO/ZnO**	**20**	**90**
6	water	GO	120	trace
7	water	nanoZnO[b]	120	70
8	water	no catalyst	240	no reaction

[a]Reaction conditions: indole (1 mmol), benzaldehyde (1 mmol), pyrrolidine (1 mmol), catalyst (wt %), and solvent (1.5 mL) were stirred at room temperature. [b]Commercially available nanoZnO. [c]Isolated yield.

In order to study the generality of the RGO/ZnO nanocatalytic system, a variety of indole substrates, aromatic aldehydes, and secondary amines were used to obtain various 3-amino alkylated indoles. The results are summarized in Table 2. It is noteworthy that all the reactions proceeded smoothly and generated 3-amino alkylated indoles in good yields (83−92%) within 15−30 min of reaction time.

Furthermore, RGO/ZnO is the best catalytic system in terms of activity, selectivity, and greenness of the protocol, with negligible waste generation from the reaction mixture. Thus, the green chemistry metrics[44,45] calculation for the model reaction provides the smaller E-factor (0.14)/process mass intensity (PMI = 1.14) and high atom economy (AE = 93.3%)/ reaction mass efficiency (RME = 84.6%) (see Supporting Information for calculations).

To study the wide applicability of the RGO/ZnO catalytic system, we further investigated the reaction of the indoles with active methylene compounds and various aromatic aldehydes to yield the corresponding 3-substituted indoles (**6a**−**6g**) via Knoevenagel condensation followed by Michael addition as shown in Scheme 2.

A model reaction of indole, benzaldehyde, and malononitrile was performed under optimized conditions, and the reaction proceeded smoothly at 50 °C and gave 3-substituted indole **6a** in excellent yield (Table 3, entry 1). The generality of reaction was studied with substituted indoles, aromatic aldehyde-bearing electron-withdrawing and -donating substituents at *ortho*, *meta*, and *para* positions, and malononitrile/ethyl 2-cyano acetate as shown in Table 3.

In general, all the reactions preceded smoothly affording 3-substituted indole derivatives in good to excellent yields. The aromatic aldehydes bearing electron-donating substituents such as −OMe and −OH at *meta* and *para* positions showed less reactivity (Table 3, entries 5−7) compared with electron-withdrawing substituents such as $-NO_2$ and chloro at *ortho* and *para* positions (Table 3, entries 2, 3, 4, and 9).

Next, we calculated the green chemistry metrics of the model reaction for the synthesis of 3-substituted indole **6a** and obtained almost the same results as compared with product **4a**, i.e., small E-factor (0.18)/process mass intensity (PMI = 1.18) and high atom economy (AE = 93.8%)/reaction mass efficiency (RME = 84.4%) (see Supporting Information for calculations).

The study was further extended to the synthesis of 2-amino-4-(indol-3-yl)-*4H*-chromenes from salicylaldehydes, indoles, and active methylene compounds such as malononitrile and ethyl 2-cyano acetate via a one-pot domino reaction involving Knoevenagel condensation, Pinner reaction, and Friedel−Crafts

Table 2. RGO/ZnO Catalyzed One-Pot Synthesis of 3-Amino Alkylated Indoles via Mannich-Type Reactions[a]

Entry	Indole (1) / Aldehyde (2) / Amine (3) / Product (4)	Product (4)	Time (min)	Yield (%)[b]
1	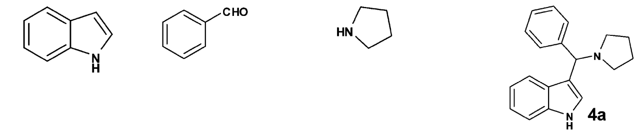	4a	20	90
2	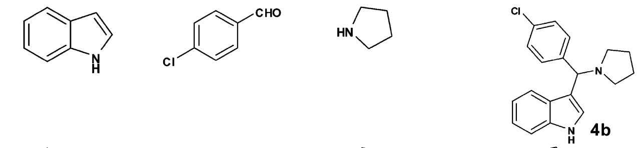	4b	25	90
3	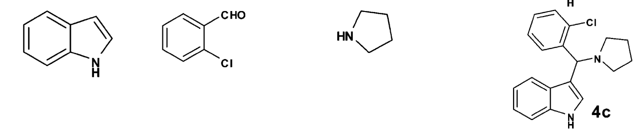	4c	30	85
4	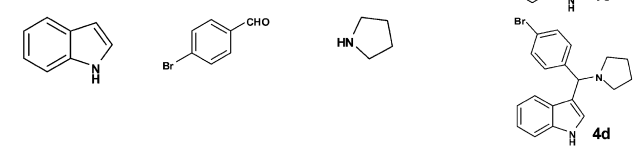	4d	20	89
5	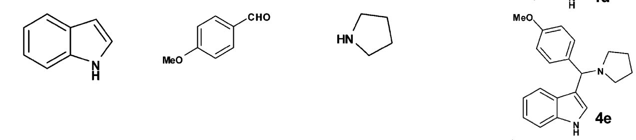	4e	20	86
6	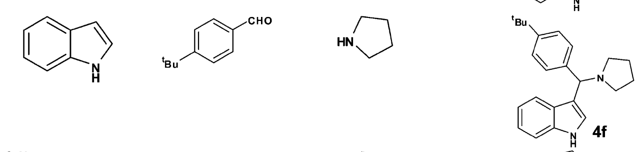	4f	20	83
7	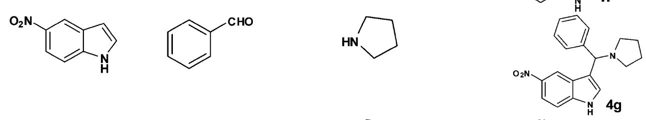	4g	30	87
8	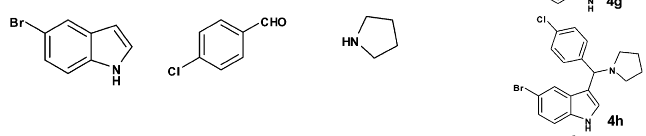	4h	25	90
9	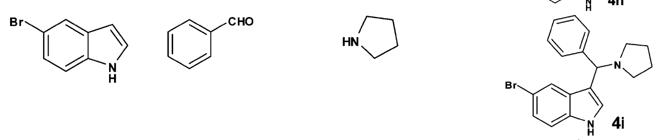	4i	30	88
10	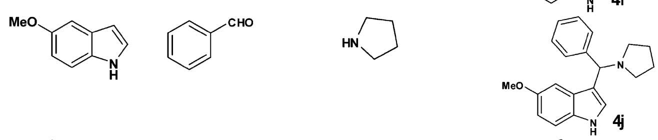	4j	30	85
11	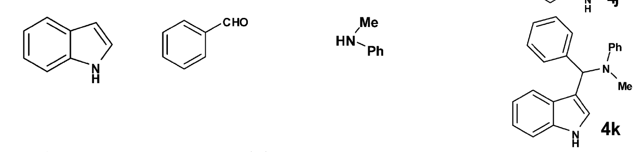	4k	20	90
12	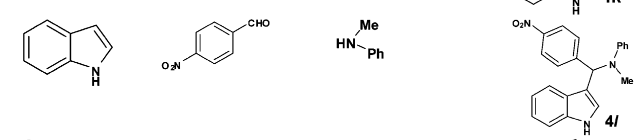	4*l*	15	92
13	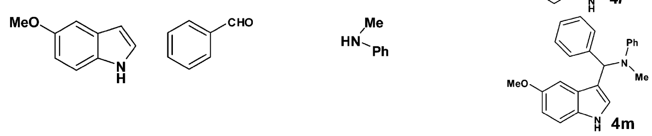	4m	15	90

[a]Reaction condition: indoles (1 mmol), aldehydes (1 mmol), secondary amines (1 mmol), RGO/ZnO (5 wt %), and water (1.5 mL) were stirred at room temperature. [b]Isolated yield.

dx.doi.org/10.1021/sc500594w | ACS Sustainable Chem. Eng. 2015, 3, 9−18

Scheme 2. RGO/ZnO Catalyzed Synthesis of 3-Substituted Indoles

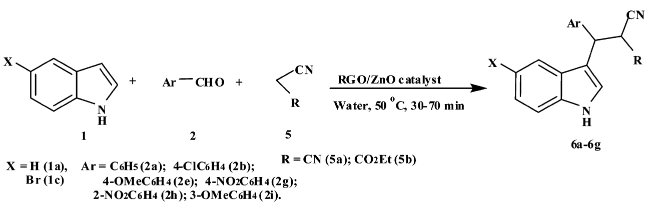

alkylation processes as depicted in Scheme 3. Almost all the reactions proceeded smoothly and produced the desired product, 2-amino-4-(indol-3-yl)-*4H*-chromenes, in good to excellent yields of 80−93% in short reaction times of 10−30 min at room temperature. The results are depicted in Table 4.

The green chemistry metrics calculation of the model reaction for the synthesis of 2-amino-4-(indol-3-yl)-*4H*-chromene **8a** gave small E-factor (0.14)/process mass intensity (PMI = 1.14) and high atom economy (AE = 94%)/reaction mass efficiency (RME = 87.5%) (see Supporting Information for calculations).

The comparison of the catalytic activity of RGO/ZnO with the reported catalysts for the synthesis of 3-substituted indoles **4a**, **6a**, and **8a** is depicted in Table 5. The results clearly indicate that the RGO/ZnO catalyst has many advantages over the reported methods in terms of high catalytic activity, mild reaction conditions, and recyclability of catalyst (Table 5).

In heterogeneous catalysis, the activity of ZnO depends on the presence of oxygen defects and high surface area as well as intrinsic properties including crystal structure, bulk composition, and morphology. We hypothesized the role of densly embeded ZnO NPs on the surface of RGO (RGO/ZnO catalyst) for Mannich, Knoevenagel, Michael, Pinner, and Friedel−Crafts alkylation reactions for the synthesis of 3-amino alkylated indoles as shown in Figure 4. In the first pathway, iminium ion formation takes place from aldehyde **2a** and pyrrolidine **3a** in the presence of active sites O^{2-} and Zn^{2+} of ZnO/RGO. The iminium ions may stabilize on the surface of the catalyst. Subsequently, indole **1a** attacks iminium ions to form an intermediate II, which can be rearranged in to the desired Mannich product **4a**.

In the second pathway, the Knoevenagel product (**7a**) can be generated from the reaction between aldehyde **1a** and malononitrile **5a** in the presence of basic site O^{2-} of ZnO on the RGO surface. Michael addition of indole **1a** on compound

Table 3. RGO/ZnO Catalyzed One-Pot Synthesis of 3-Substituted Indoles[a]

Entry	Indole (**1**)	Aldehyde (**2**)	R (**5**)	Product (**6**)	Time (min)	Yield (%)[b]
1	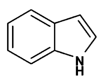	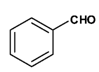	CN	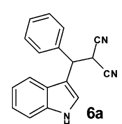 6a	40	90
2	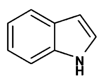	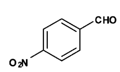	CN	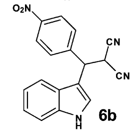 6b	30	95
3	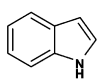	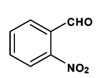	CN	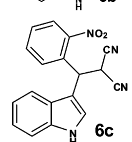 6c	35	87
4	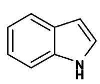	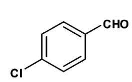	CN	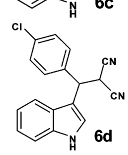 6d	30	92
5	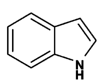	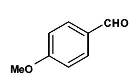	CN	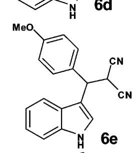 6e	60	85
6	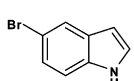	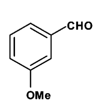	CO_2Et	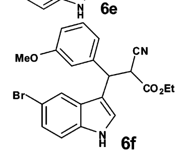 6f	70	82[c]
7	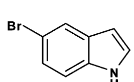	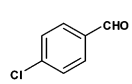	CN	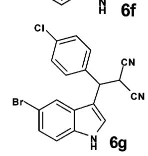 6g	40	91

[a]Reaction condition: indoles (1 mmol), aldehydes (1 mmol), malononitrile/ethyl 2-cyano acetate (1 mmol), RGO/ZnO (5 wt %), and water (1.5 mL) were stirred at 50 °C. [b]Isolated yield. [c]Isolated yield of racemic mixture (50:50 diastereomers).

Scheme 3. RGO/ZnO Catalyzed Synthesis of 2-Amino-4-(indol-3-yl)-4*H*-chromenes in Water

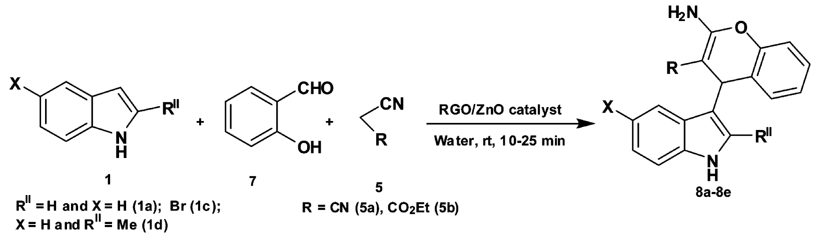

Table 4. RGO/ZnO-Catalyzed One-Pot Synthesis of 2-Amino-4-(indol-3-yl)-4*H*-chromenes[a]

Entry	Indole (**1**)	R (**5**)	Product (**8**)	Time (min)	Yield (%)[b]
1	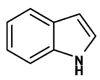	CN	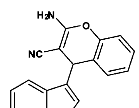 8a	15	93
2	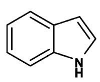	CO_2Et	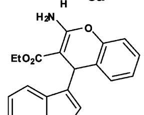 8b	25	85
3	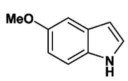	CN	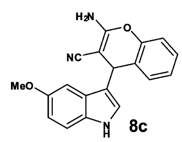 8c	12	87
4	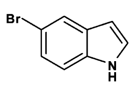	CN	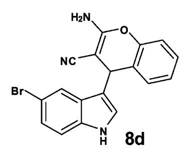 8d	15	90
5	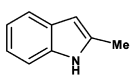	CN	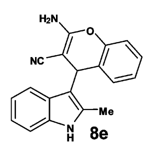 8e	10	97

[a]Reaction condition: indoles (1 mmol), salicylaldehydes (1 mmol), malononitrile/ethyl 2-cyano acetate (1 mmol), RGO/ZnO (5 wt %), and water (1.5 mL) were stirred at room temperature. [b]Isolated yield.

Table 5. Comparison of Catalytic Activity of RGO/ZnO with Reported Catalysts for Synthesis of 3-Substituted Indoles 4a, 6a, and 8a

entry	product	catalyst	time (h)	temp. (°C)	yield (%)	ref	recyclability
1	**4a**	L-proline	5.5	rt	87	29	no
2	**4a**	SDS	2	80	78	30	no
3	**4a**	**RGO/ZnO**	**0.3**	**rt**	**90**	**present**	yes
4	**6a**	TBAF·3H_2O	2	60	85	35	no
5	**6a**	Cu-L salen complex/KH_2PO_4	6	60	90	32	no
6	**6a**	**RGO/ZnO**	**0.6**	**50**	**90**	**present**	yes
7	**8a**	TBAF·3H_2O	3	60	88	35	no
8	**8a**	$Zn(ClO_4).6H_2O/NaBAr_F$	26	rt	87	34	no
9	**8a**	**RGO/ZnO**	**0.25**	**rt**	**93**	**present**	yes

7a can be enhanced by Zn^{2+} of ZnO upon activation of olefinic compound **7a** to form 3-substituted indole **6a** (Figure 4).

In the third pathway, iminochromene intermediate (**V**) can be generated from the Knoevenagel condensation of salicylaldehyde **7** with malononitrile **5a** followed by a Pinner reaction in the presence of active sites O^{2-} and Zn^{2+} of the ZnO/RGO catalyst. Subsequently, Friedel–Crafts alkylation of indole with iminochromene intermediate can result in the

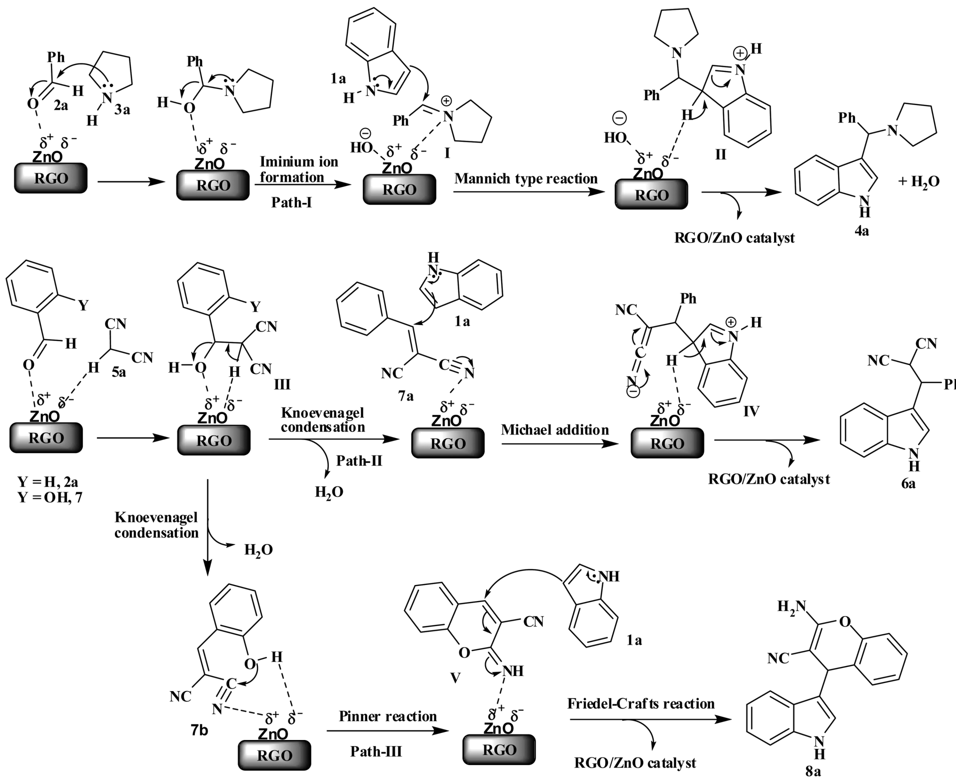

Figure 4. Plausible mechanism of RGO/ZnO-catalyzed one-pot synthesis of 3-substituted indoles.

formation of 2-amino-4-(indol-3-yl)-*4H*-chromene **8a** (Figure 4).

The recyclability of the the RGO/ZnO catalyst was studied in the one-pot synthesis of 3-amino alkylated indole **4a** under the optimized conditions. No significant loss in catalytic activity was observed after 6 runs (Figure 5).

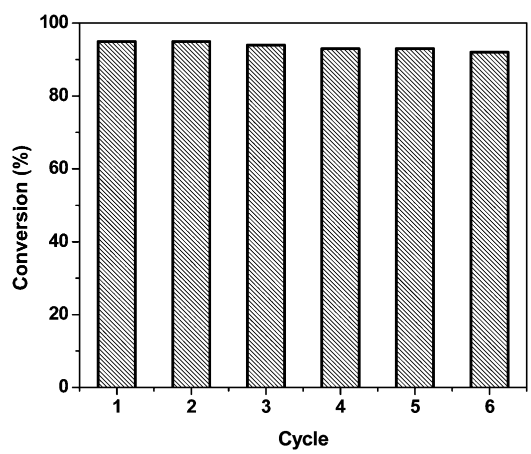

Figure 5. Recycling study of RGO/ZnO catalyst for synthesis of 3-amino alkylated indole **4a**.

CONCLUSION

In summary, it was demonstrated that RGO/ZnO composites act as highly efficient and reusable heterogeneous catalysts in the one-pot three component synthesis of various 3-substituted indoles. The RGO/ZnO catalytic system provides advantages such as high catalytic efficiency, high yields in short reaction times, applicability to a wide range of indole-based organic reactions, and use of water as a green solvent. The RGO/ZnO catalyst can be easily recovered from reaction mixtures and recycled at least six times without significant loss in catalytic activity. Furthermore, we have developed a green method for the synthesis of various 3-substituted indoles with higher environmental compatibility and sustainability factors such as smaller E-factor and higher atom economy.

EXPERIMENTAL SECTION

General Procedure for Synthesis of 3-Amino Alkylated indoles (4a–4m). A mixture of indole (**1**, 1 mmol), aldehydes (**2**, 1 mmol), secondary amines (**3**, 1 mmol), RGO/ZnO catalyst (5 wt %), and water (1.5 mL) were placed in a 10 mL round-bottomed flask and stirred at room temperature. After completion of the reaction (monitored by TLC), water was decanted from reaction mixture, and EtOH was added to the reaction mixture followed by centrifuging to separate the solid catalyst. The organic layer was dried over Na_2SO_4, and the solvent was removed under reduced pressure. The obtained crude product was purified by recrystallization from diethyl ether/*n*-hexane. All compounds were characterized by MP, NMR, IR, mass spectral data.

3-((4-Bromophenyl)(pyrrolidin-1-yl)methyl)-1H-indole (**4d**). White crystals; mp 146–148 °C. IR (KBr) 3415, 2966, 2794, 1483, 1346, 1219, 1097, 1007, 743 cm^{-1}. ^{1}H NMR (400 MHz, $CDCl_3$) δ (ppm) 8.03, (br s, 1H), 7.78 (d, *J* = 7.9 Hz, 1H), 7.43 (d, *J* = 8.5 Hz, 2H), 7.37 (d, *J* = 8.5 Hz, 2H), 7.31 (d, *J* = 7.9 Hz, 1H), 7.18–7.16 (m, 2H), 7.09 (t, *J* = 7.9 Hz, 1H), 4.56 (s, 1H), 2.50 (d, *J* = 6.7 Hz, 4H), 1.77 (s, 4H). ^{13}C NMR (100 MHz, $CDCl_3$) δ (ppm) 143.80, 136.40, 131.47, 129.62, 126.48, 122.27, 122.10, 120.34, 119.99, 119.74, 111.30, 67.52, 53.77, 23.78. HRMS (ES): Calcd 354.0732, found 354.0732. Anal. Calcd for $C_{19}H_{19}BrN_2$: C, 64.23; H, 5.39; N, 7.89. Found: C, 64.24; H, 5.39; N, 7.90

3-((4-Methoxyphenyl)(pyrrolidin-1-yl)methyl)-1H-indole (**4e**). White crystals; mp 173–175 °C. IR (KBr) 3420, 3042, 2828, 1487, 1343, 1217, 1159, 750 cm^{-1}. ^{1}H NMR (400 MHz, $CDCl_3$) δ (ppm) 8.18 (br s, 1H), 7.82 (d, *J* = 7.32 Hz, 1H), 7.47 (d, *J* = 8.5 Hz, 2H), 7.28 (d, J = 7.9 Hz, 1H), 7.16 (t, J = 7.9 Hz, 2H), 7.10 (t, J = 7.3 Hz, 1H), 6.82 (d, J = 8.5 Hz, 2H), 4.59 (s, 1H), 3.76 (s, 3H), 2.56−2.46 (m, 4H), 1.79 (s, 4H). ^{13}C NMR (100 MHz, $CDCl_3$) δ (ppm) 158.49, 137.01, 136.44, 129.02, 126.79, 122.08, 120.08, 120.02, 119.56, 113.79, 111.30, 67.55, 55.49, 53.94, 23.81. HRMS (ES): Calcd 306.1732, found 306.1733. Anal. Calcd for $C_{20}H_{22}N_2O$: C, 78.40; H, 7.24; N, 9.14. Found: C, 78.41; H, 7.23; N, 9.14

3-((4-(tert-Butyl)phenyl)(pyrrolidin-1-yl)methyl)-1H-indole (***4f***). White solid; mp 124−126 °C. IR (KBr) 3417, 2962, 2795, 1507, 1455, 1295, 1216, 1116, 738 cm^{-1}. ^{1}H NMR (400 MHz, $CDCl_3$) δ (ppm) 8.05 (br s, 1H), 7.85 (d, J = 9.1 Hz, 1H), 7.45 (d, J = 7.9 Hz, 2H), 7.30 (d, J = 7.9 Hz, 1H), 7.26−7.23 (m, 3H), 7.14 (t, J = 7.3 Hz, 1H), 7.09 (t, J = 7.9 Hz, 1H), 4.55 (s, 1H), 2.52−2.46 (m, 4H), 1.77 (s, 4H), 1.26 (s, 9H). ^{13}C NMR (100 MHz, $CDCl_3$) δ (ppm) 149.54, 141.72, 136.39, 127.58, 126.93, 125.37, 122.24, 122.10, 120.13, 120.01, 119.59, 111.35, 68.08, 54.21, 34.68, 31.72, 23.84. HRMS (ES): Calcd 332.2252, found 332.2252. Anal. Calcd for $C_{23}H_{28}N_2$: C, 83.09; H, 8.49; N, 8.43. Found: C, 83.09; H, 8.50; N, 8.43

5-Bromo-3-((4-chlorophenyl)(pyrrolidin-1-yl)methyl)-1H-indole (***4h***). Off white solid; mp 142−144 °C. IR (KBr) 3434, 2926, 2794, 1563, 1482, 1214, 1091, 748 cm^{-1}. ^{1}H NMR (400 MHz, $CDCl_3$) δ (ppm) 8.09 (br s, 1H), 7.93 (s, 1H), 7.44 (d, J = 8.5 Hz, 2H), 7.22 (d, J = 8.5 Hz, 3H), 7.16−7.14 (m, 2H), 4.48 (s, 1H), 2.47 (d, J = 5.0 Hz, 4H), 1.76 (s, 4H). ^{13}C NMR (100 MHz, $CDCl_3$) δ (ppm) 143.00, 135.09, 132.53, 129.19, 128.73, 128.26, 125.26, 123.34, 122.58, 119.35, 113.21, 112.83, 67.50, 53.87, 23.85. HRMS (ES): Calcd 388.0342, found 388.0343. Anal. Calcd for $C_{19}H_{18}BrClN_2$: C, 58.56; H, 4.66; N, 7.19. Found: C, 58.55; H, 4.66; N, 7.18

5-Methoxy-3-(phenyl(pyrrolidin-1-yl)methyl)-1H-indole (***4j***). Off white solid; mp 117−119 °C. IR (KBr) 3418, 2924, 2791, 1583, 1478, 1447, 1212, 1031, 749 cm^{-1}. ^{1}H NMR (400 MHz, $CDCl_3$) δ (ppm) 8.03 (br s, 1H), 7.61 (d, J = 7.3 Hz, 2H), 7.36−7.32 (m, 2H), 7.31 (s, 1H), 7.25−7.23 (m, 2H), 6.88 (dd, J = 9.1 Hz, J = 2.4 Hz, 1H), 4.61 (s, 1H), 3.92 (s, 3H), 2.60−2.63 (m, 4H), 1.85 (s, 4H). ^{13}C NMR (100 MHz, $CDCl_3$) δ (ppm) 154.12, 144.74, 131.68, 128.45, 127.96, 127.26, 126.83, 123.08, 119.58, 112.05, 111.87, 102.40, 68.31, 56.22, 53.91, 23.86. HRMS (ES): Calcd 306.1732, found 306.1733. Anal. Calcd for $C_{20}H_{22}N_2O$: C, 78.40; H, 7.24; N, 9.14. Found: C, 78.41; H, 7.25; N, 9.14

General Procedure for Synthesis of 3-Substituted Indoles (6a−6g) and (8a−8e). A mixture of indole (**1**, 1 mmol), aldehyde/o-hydroxy aldehyde (**2**/**7**, 1 mmol), active methylene compound (**5**, 1 mmol), RGO/ZnO catalyst (5 wt %), and water (1.5 mL) were placed in a 10 mL round-bottomed flask and stirred at room temperature/50 °C. After completion of the reaction (monitored by TLC), water was decanted from reaction mixture, and EtOH was added to the reaction mixture followed by centrifuging to separate the solid catalyst. The organic layer was dried over Na_2SO_4, and the solvent was removed under reduced pressure. The obtained crude product was purified by recrystallization from diethyl ether or EtOAc/*n*-hexane.

Ethyl3-(5-bromo-1H-indol-3-yl)-2-cyano-3-(3-methoxyphenyl)-propanoate (***6f***). Off white solid; mp 72−74 °C. IR (KBr) 3411, 2937, 2836, 2251, 1736, 1600, 1490, 1459, 1369, 1320, 1262, 1155, 1107, 1031, 885, 856, 797, 778, 761, 697, 586 cm^{-1}. ^{1}H NMR (400 MHz, $CDCl_3$) δ (ppm) 8.43 (br s, 0.5H, NH), 8.38 (brs, 0.5H, NH), 7.53−7.48 (m, 2H), 7.23 (d, J = 8.5 Hz, 3H), 7.03 (d, J = 7.3 Hz, 0.5H), 6.96 (s, 1H), 6.88 (s, 0.5H), 6.84−6.79 (t, J = 9.1 Hz, 1H), 5.00 (d, J = 6.1 Hz, 0.5H), 4.93 (d, J = 6.7 Hz, 0.5H), 4.26 (d, J = 6.7 Hz, 0.5H), 4.17 (d, J = 6.7 Hz, 0.5H), 4.13 (t, J = 6.7 Hz, 2H), 3.77 (s, 1.5H), 3.75 (s, 1.5H), 1.12 (q, J = 7.3 Hz, 3H). ^{13}C NMR (100 MHz, $CDCl_3$) δ (ppm) 165.11, 159.87, 140.84, 139.69, 134.79, 129.81, 125.43, 123.40, 121.33, 121.15, 120.08, 114.24, 114.06, 113.26, 112.78, 63.03, 55.20, 45.02, 42.78, 13.73. HRMS (ES): Calcd 426.0579, found 426.0578. Anal. Calcd for $C_{21}H_{19}BrN_2O_3$: C, 59.03; H, 4.48; N, 6.56. Found: C, 59.04; H, 4.47; N, 6.55.

2-((5-Bromo-1H-indol-3-yl)(4-chlorophenyl)methyl)malononitrile (***6g***). Pale yellow solid; mp 148−151 °C. IR (KBr) 3347, 3032, 2934, 2881, 2371, 2345, 2259, 2228, 1900, 1595, 1508, 1490, 1465, 1451, 1426, 1412, 1350, 1321, 1282, 1253, 1227, 1196, 1141, 1115, 1097, 1016, 936, 823, 749, 769, 782, 641 cm^{-1}. ^{1}H NMR (400 MHz, $CDCl_3$) δ (ppm) 8.42 (br s, 1H), 7.41−7.29 (m, 7H), 4.84 (d, J = 6.1 Hz, 1H), 4.39 (d, J = 6.1 Hz, 1H). ^{13}C NMR (100 MHz, $CDCl_3$) δ (ppm) 135.34, 135.18, 132.16, 130.36, 129.85, 129.80, 127.74, 126.61, 123.53, 121.40, 114.06, 113.45, 112.11, 111.91, 43.59, 29.83. HRMS (ES): Calcd 382.9825, found 382.9820. Anal. Calcd for $C_{18}H_{11}BrClN_3$: C, 56.20; H, 2.88; N, 10.92. Found: C, 56.20; H, 2.87; N, 10.92

2-Amino-4-(5-bromo-1H-indol-3-yl)chroman-3-carbonitrile (***8d***). Yellow solid; mp 178−181 °C. IR (KBr) 3446, 3383, 3321, 3242, 3204, 3081, 2851, 2345, 2371, 2197, 1660, 1610, 1581, 1490, 1448, 1458, 1421, 1403, 1331, 1272, 1259, 1228, 1077, 1099, 1043, 847, 883, 793, 750, 582, 523 cm^{-1}. ^{1}H NMR (400 MHz, $CDCl_3$) δ (ppm) 8.19 (br s, 1H), 7.38 (br s, 1H), 7.21−7.15 (m, 4H), 7.04−6.96 (m, 3H), 5.01 (s, 1H), 4.61 (s, 2H). ^{13}C NMR (100 MHz, $CDCl_3$) δ (ppm) 159.57, 148.71, 135.84, 129.64, 128.54, 127.53, 125.42, 124.12, 122.59, 121.81, 120.42, 118.84, 116.58, 113.12, 60.49, 32.70. HRMS (ES): Calcd 367.0320, found 367.0322. Anal. Calcd for $C_{18}H_{14}BrN_3O$: C, 58.71; H, 3.83; N, 11.41. Found: C, 58.72; H, 3.83; N, 11.41.

■ ASSOCIATED CONTENT

Supporting Information

Solvent relaxation calculations using NMR method, TEM image of recycled RGO/ZnO, green chemistry metrics calculations, and ^{1}H and ^{13}C NMR spectra of selected compounds. This material is available free of charge via the Internet at http://pubs.acs.org.

■ AUTHOR INFORMATION

Corresponding Authors

*Fax: 0261255476. Tel: 026125 9296. E-mail: takuya.tsuzuki@anu.edu.au (T.T.).

*Fax: 91-11-27667501. Tel: 91-11-27662683. E-mail: dsrawat@chemistry.du.ac.in (D.S.R).

Author Contributions

J.W. and T.T. synthesized RGO/ZnO composite materials. D.S.R. and U.C.R. analyzed catalytic properties of RGO/ZnO composite materials. All authors contributed to data interpretation. S.P. measured the surface area of the GO/ZnO composite using the solvent relaxation NMR method.

Notes

The authors declare no competing financial interest.

■ ACKNOWLEDGMENTS

D.S.R. acknowledges a R&D Grant, University of Delhi, Delhi, India for financial support. U.C.R. is thankful to UGC for the award of a senior research fellowship. D.S.R. and U.C.R. thank USIC−CIF, University of Delhi, for assisting in acquiring analytical data. T.T. and J.W. acknowledge the assistance from Deakin University Microscopy Centre for the TEM study.

■ REFERENCES

(1) Zhu, Y.; Murali, S.; Cai, W.; Li, X.; Suk, J. W.; Potts, J. R.; Ruoff, R. S. Graphene and graphene oxide: synthesis, properties, and applications. *Adv. Mater.* **2010**, *22*, 3906−3924.

(2) Geim, A. K. Graphene: Status and prospects. *Science* **2009**, *324*, 1530−1534.

(3) Gilje, S.; Han, S.; Wang, M.; Wang, K. L.; Kaner, R. B. A chemical route to graphene for device applications. *Nano Lett.* **2007**, *7*, 3394−3398.

(4) Shao, Y.; Wang, J.; Wu, H.; Liu, J.; Aksay, I. A.; Lin, Y. Graphene based electrochemical sensors and biosensors: A review. *Electroanalysis* **2010**, *22*, 1027−1036.

(5) Chen, S.; Zhu, J.; Wu, X.; Han, Q.; Wang, X. Graphene oxide−MnO_2 nanocomposites for supercapacitors. *ACS Nano* **2010**, *4*, 2822−2830.

(6) Chandra, V.; Park, J.; Chun, Y.; Lee, J. W.; Hwang, I. C.; Kim, K. S. Water-dispersible magnetite-reduced graphene oxide composites for arsenic removal. *ACS Nano* **2010**, *4*, 3979−3986.
(7) Pyun, J. Graphene oxide as catalyst: Application of carbon materials beyond nanotechnology. *Angew. Chem.* **2011**, *50*, 46−48.
(8) Li, Y.; Gao, W.; Ci, L.; Wang, C.; Ajayan, P. M. Catalytic performance of Pt nanoparticles on reduced graphene oxide for methanol electro-oxidation. *Carbon* **2010**, *48*, 1124−1130.
(9) Dreyer, D. R.; Jia, H. P.; Bielawski, C. W. Graphene oxide: A convenient carbocatalyst for facilitating oxidation and hydration reactions. *Angew. Chem.* **2010**, *122*, 6965−6968.
(10) Gao, Y.; Ma, D.; Wang, C.; Guan, J.; Bao, X. Reduced graphene oxide as a catalyst for hydrogenation of nitrobenzene at room temperature. *Chem. Commun.* **2011**, *47*, 2432−2434.
(11) Li, J.; Liu, C.; Liu, Y. Au/graphene hydrogel: Synthesis, characterization and its use for catalytic reduction of 4-nitrophenol. *J. Mater. Chem.* **2012**, *22*, 8426−8430.
(12) Scheuermann, G. M.; Rumi, L.; Steurer, P.; Bannwarth, W.; Mulhaupt, R. Palladium nanoparticles on graphite oxide and its functionalized graphene derivatives as highly active catalysts for the Suzuki−Miyaura coupling reaction. *J. Am. Chem. Soc.* **2009**, *131*, 8262−8270.
(13) Chen, Y. L.; Hu, Z. A.; Chang, Y. Q.; Wang, H. W.; Zhang, Z. Y.; Yang, Y. Y.; Wu, H. Y. Zinc oxide/reduced graphene oxide composites and electrochemical capacitance enhanced by homogeneous incorporation of reduced graphene oxide sheets in zinc oxide matrix. *J. Phys. Chem. C* **2011**, *115*, 2563−2571.
(14) Li, B.; Cao, H. ZnO/graphene composite with enhanced performance for the removal of dye from water. *J. Mater. Chem.* **2011**, *21*, 3346−3349.
(15) Shin, K. S.; Jo, H.; Shin, H. J.; Choi, W. M.; Choi, J. Y.; Kim, S. W. High quality graphene-semiconducting oxide heterostructure for inverted organic photovoltaics. *J. Mater. Chem.* **2012**, *22*, 13032−13038.
(16) Xu, T.; Zhang, L.; Cheng, H.; Zhu, Y. Significantly enhanced photocatalytic performance of ZnO *via* graphene hybridization and the mechanism study. *Appl. Catal., B* **2011**, *101*, 382−387.
(17) Kumar, A.; Saxenaa, D.; Gupta, M. K. Nanoparticle catalyzed reaction (NPCR): ZnO-NP catalyzed Ugi-reaction in aqueous medium. *Green Chem.* **2013**, *15*, 2699−2703.
(18) Ghosh, P. P.; Das, A. R. Nanocrystalline and reusable ZnO catalyst for the assembly of densely functionalized 4*H*-Chromenes in aqueous medium *via* one-pot three component reactions: A greener "NOSE" approach. *J. Org. Chem.* **2013**, *78*, 6170−6181.
(19) Chanda, A.; Fokin, V. V. Organic Synthesis "On Water. *Chem. Rev.* **2009**, *109*, 725−748.
(20) Simon, M. O.; Li, C. J. Green chemistry oriented organic synthesis in water. *Chem. Soc. Rev.* **2012**, *41*, 1415−1427.
(21) Breslow, R. Hydrophobic effects on simple organic reactions in water. *Acc. Chem. Res.* **1991**, *24*, 159−165.
(22) Ye, X.; Fernando, S.; Wilson, W.; Singh, A. Application of amphiphilic catalysts, ultrasonication, and nanoemulsions for biodiesel production process. *Chem. Eng. Technol.* **2007**, *30*, 1481−1487.
(23) Wang, J.; Tsuzuki, T.; Tang, B.; Cizek, P.; Sun, L.; Wang, X. Synthesis of silica-coated ZnO nanocomposite: The resonance structure of polyvinyl pyrrolidone (PVP) as a coupling agent. *Colloid Polym. Sci.* **2010**, *288*, 1705−1711.
(24) Wang, J.; Tsuzuki, T.; Tang, B.; Sun, L.; Dai, X. J.; Rajmohan, G. D.; Li, J.; Wang, X. Recyclable textiles functionalized with reduced graphene oxide@ZnO for removal of oil spills and dye pollutants. *Aust. J. Chem.* **2014**, *67*, 71−77.
(25) Casapullo, A.; Bifulco, G.; Bruno, I.; R. New bisindole alkaloids of the topsentin and hamacanthin classes from the mediterranean marine sponge *Rhaphisia lacazei*. *J. Nat. Prod.* **2000**, *63*, 447−451.
(26) Horgen, F. D.; Santos, D. B. D.; Goetz, G.; Sakamoto, B.; Kan, Y.; Nagai, H.; Scheuer, P. J. A new depsipeptide from the sacoglossan mollusk *Elysia ornata* and the green alga *Bryopsis* species. *J. Nat. Prod.* **2000**, *63*, 152−154.
(27) Deng, J.; Sanchez, T.; Neamati, N.; Briggs, J. M. Dynamic pharmacophore model optimization: identification of novel HIV-1 integrase inhibitors. *J. Med. Chem.* **2006**, *49*, 1684−1692.
(28) Contractor, R.; Samudio, I. J.; Estrov, Z.; Harris, D.; McCubrey, J. A.; Safe, S. H.; Andreeff, M.; Konopleva, M. A novel ring-substituted diindolylmethane, 1,1-bis[3′-(5-methoxyindolyl)]-1-(*p*-t-butylphenyl) methane, inhibits extracellular signal-regulated kinase activation and induces apoptosis in acute myelogenous leukemia. *Cancer Res.* **2005**, *65*, 2890−2898.
(29) Kumar, A.; Gupta, M. K.; Kumar, M. L-Proline catalysed multicomponent synthesis of 3-amino alkylated indoles *via* a Mannich-type reaction under solvent-free conditions. *Green Chem.* **2012**, *14*, 290−295.
(30) Kumar, A.; Gupta, M. K.; Kumar, M.; Saxena, D. Micelle promoted multicomponent synthesis of 3-amino alkylated indoles *via* a Mannich-type reaction in water. *RSC Adv.* **2013**, *3*, 1673−1678.
(31) Rajesh, U. C.; Kholiya, R.; Pavan, V. S.; Rawat, D. S. Catalyst free, ethylene glycol promoted one-pot three component synthesis of 3-amino alkylated indoles via Mannich-type. *Tetrahedron Lett.* **2014**, *55*, 2977.
(32) Qu, Y.; Ke, F.; Zhou, L.; Li, Z.; Xiang, H.; Wu, D.; Zhou, X. Synthesis of 3-indole derivatives by copper sulfonato salen catalyzed three-component reactions in water. *Chem. Commun.* **2011**, *47*, 3912−3914.
(33) Anselmo, D.; Adán, E. C. E.; Belmonte, M. M.; Kleij, A. W. Zn-Mediated synthesis of 3-substituted indoles using a three-component reaction approach. *Eur. J. Inorg. Chem.* **2012**, 4694−4700.
(34) Chen, W.; Cai, Y.; Fu, X.; Liu, X.; Lin, L.; Feng, X. Enantioselective one-pot synthesis of 2-amino-4-(indol-3-yl)-4*H*-chromenes. *Org. Lett.* **2011**, *13*, 4910−4913.
(35) Singh, N.; Allam, B. K.; Raghuvanshi, D. S.; Singh, K. N. An efficient tetrabutylammonium fluoride (TBAF)-catalyzed three-component synthesis of 3-substituted indole derivatives under solvent-free conditions. *Adv. Synth. Catal.* **2013**, *355*, 1840−1848.
(36) Arya, K.; Rajesh, U. C.; Rawat, D. S. Proline confined FAU zeolite: Heterogeneous hybrid catalyst for the synthesis of spiroheterocycles *via* a Mannich type reaction. *Green Chem.* **2012**, *14*, 3344−3351.
(37) Thakur, A.; Tripathi, M.; Rajesh, U. C.; Rawat, D. S. Ethylenediammonium diformate (EDDF) in PEG600: An efficient ambiphilic novel catalytic system for the one-pot synthesis of 4H-pyrans *via* Knoevenagel condensation. *RSC Adv.* **2013**, *3*, 18142−18148.
(38) Rajesh, U. C.; Manohar, S.; Rawat, D. S. Hydromagnesite as an efficient recyclable heterogeneous solid base catalyst for the synthesis of flavanones, flavonols and 1,4-dihydropyridines in water. *Adv. Synth. Catal.* **2013**, *355*, 3170.
(39) Rajesh, U. C.; Divya.; Rawat, D. S. Functionalized superparamagnetic Fe_3O_4 as an efficient quasi-homogeneous catalyst for multi-component reactions. *RSC Advances* **2014**, *4*, 41323.
(40) Manohar, S.; Rajesh, U. C.; Khan, S. I.; Tekwani, B. L.; Rawat, D. S. Novel 4-aminoquinoline-pyrimidine based hybrids with improved in vitro and in vivo antimalarial activity. *ACS Med. Chem. Lett.* **2012**, *3*, 555−559.
(41) Atheaya, H.; Khan, S. I.; Mamgain, R.; Rawat, D. S. Synthesis, thermal stability, antimalarial activity of symmetrically and asymmetrically substituted tetraoxanes. *Bioorg. Med. Chem. Lett.* **2008**, *18*, 1446−1449.
(42) Beena; Kumar, N.; Rohilla, R. K.; Roy, N.; Rawat, D. S. Synthesis and antibacterial activity evaluation of metronidazole−triazole conjugates. *Bioorg. Med. Chem. Lett.* **2009**, *19*, 1396−1398.
(43) Wang, J.; Tsuzuki, T.; Tang, B.; Hou, X.; Sun, L.; Wang, X. Reduced graphene oxide/ZnO composite: Reusable adsorbent for pollutant management. *ACS Appl. Mater. Interfaces* **2012**, *4*, 3084−3090.
(44) McGonagle, F. I.; Sneddon, H. F.; Jamieson, C.; Watson, A. J. B. Molar efficiency: A useful metric to gauge relative reaction efficiency in discovery medicinal chemistry. *ACS Sustainable Chem. Eng.* **2014**, *2*, 523−532.

(45) Sheldon, R. A. E factors, green chemistry and catalysis: An odyssey. *Chem. Commun.* **2008**, 3352−3365.